Sound Contrast Imaging Using Uniform Ring Configuration of Transducers with L1 Reconstruction

Conference Paper · October 2015

DOI: 10.1109/ATC.2015.7388308

2 authors:

Tran Quang-Huy .
HPU2 - Hanoi Pedagogical University No2
7 PUBLICATIONS **1** CITATION
SEE PROFILE

Duc-Tan Tran
Vietnam National University, Hanoi
125 PUBLICATIONS **118** CITATIONS
SEE PROFILE

Sound Contrast Imaging Using Uniform Ring Configuration of Transducers with l_1 Reconstruction

Tran Quang-Huy†, Tran Duc-Tan‡
†Faculty of Physics, Hanoi Pedagogical University No2, Hanoi, VIETNAM
‡Faculty of Electronics & Telecommunications, VNU University of Engineering & Technology, Hanoi, VIETNAM
E-mail: tranquanghuy @hpu2.edu.vn, tantd@vnu.edu.vn

***Abstract*— Ultrasound tomography offers the potential for detecting of very small tumors whose sizes are smaller than the wavelength of the incident pressure wave without ionizing radiation. Based on inverse scattering technique, this imaging modality uses some material properties such as sound contrast and attenuation in order to detect small objects. One of the most commonly used methods in ultrasound tomography is the Distorted Born Iterative Method (DBIM). The compressed sensing technique was applied in the DBIM as a promising approach for the image reconstruction quality improvement. Nevertheless, the random measurement configuration of transducers in this method is very difficult to set up in practice. Therefore, in this paper, we take advantages of simpler sparse uniform measurement configuration set-up of transducers and high-quality image reconstruction of l_1 non-linear regularization in sparse scattering domain. The simulation results demonstrate the high performance of the proposed approach in terms of tremendously reduced total runtime and normalized error.**

Keywords—Ultrasound tomography, inverse scattering, Distorted Born iterative method (DBIM), sparse uniform ring configuration (SC), l_1 regularization.

I. INTRODUCTION

According to the World Health Organization (WHO), every year, there are approximately 10 million women in the world dying of breast cancer. If the cancer is early detected, it can significantly improve survival, about 25%. Therefore, imaging techniques of strange tumors when they are small (i.e. the diameter of tumors smaller than 5 mm) is essential. Mammography technique is widely used to identify breast cancer in postmenopausal women. However, for women under 50 years of age, this imaging technique is limited because the breast tissues of these women are dense. The dense tissues do not provide the sound contrast needed to create the image of small tumors. Meanwhile, ultrasound tomography technique, based on inverse scattering theory, can overcome this problem. It is an alternative modality to mammography in breast cancer diagnosis.

Ultrasound-based imaging technique uses sound waves with frequencies in the range of 1-20 MHz. Ultrasound wave transmits through tissues in body and it will be scattered when it encounters object (i.e. strange tumor) whose size is smaller than the wavelength of the incident wave. In principle, scattering rays will be emitted in all directions from the object. Thereafter, scattering signal is collected by receivers and is converted into an electrical signal. This signal is displayed on the screen after it has been amplified and processed. Image created by the ultrasound scanner is called ultrasound imaging, or ultrasonography. Nowadays, ultrasound imaging is widely used in practice due to its noninvasive nature, low cost, capability of forming real time imaging, and the continuing improvements in image quality. It is commonly used for imaging organs and soft tissue structures in human body.

Imaging techniques, based on inverse scattering theory, have high computational complexity that is the greatest hurdle to the release of the ultrasound-tomography device commercialization. Therefore, inverse scattering techniques mostly concentrate to the reduction of the computational complexity and improvement of imaging quality. Inverse scattering problem involves estimation of the distribution of the acoustical scattering parameters (i.e. speed of sound, attenuation, density and others) which are solved by inverting the wave equation of the inhomogeneous environment. Thus, ultrasound tomography shows the quantitative information of the object under examination. Currently, there are just several ultrasonic-computed tomography devices, such as CURE [1, 2], HUTT [3], and TMS [4]. The first two-devices are limited by the spatial resolution and accuracy due to the elimination of diffraction problem, but the third device offers more accurate results due to using the inverse scattering algorithms. Most of research works on ultrasound tomography are based on Born approximation. Born Iterative Method (BIM) and Distorted Born Iterative Method (DBIM) are well-known for diffraction tomography [5].

Compressed sensing (CS), which is introduced by Candes and Tao [6] and Donoho [7] in 2006, could acquire and reconstruct sparse signals at a rate lower than that of Nyquist. Random measurement approach in the detection geometry configuration is proposed in [8]. A set of measurements of the scattered field is performed using sets of receiver's random positions. This method can reduce the computational complexity and improve the quality of the reconstruction of the sound contrast. However, this method does not denoise well and is difficult to set up in practice. Motivated by the simpler hardware implementation for the measurement configuration in ultrasound tomography, in this paper, we take advantages of simpler uniform measurement configuration set-up of transducers and high-quality image reconstruction of l_1 non-linear regularization [12]. With compressed sensing, the random measurement configuration of transducers is required. This configuration results the difficult hardware implementation in practical applications. Meanwhile, we propose to use the sparse uniform ring configuration (SC)

978-1-4673-8374-5/15/$31.00 ©2015 IEEE

which provides a very simple hardware implementation. Furthermore, the l_1 non-linear regularization is used in the image reconstruction process that is a powerful solver for the sparse problem. So, we take into account the sparse scattering domain by using a very small number of transducers. As a result, this approach (SC-DBIM) offers a very high performance, compared to the conventional DBIM method.

II. Distorted Born Iterative Method

A measurement configuration is set up for tranducers T-R (i.e. transmitters and receivers), located in a circle around the object in order to obtain the scattered data (see Fig.1). Each tranducer can both transmit and receive. At an instance, only one transmitter and one receiver are active to for a corresponding measured data value. This data was processed using DBIM to reconstruct the sound contrast of scatters. In this way, any tissue can be detected in this medium.

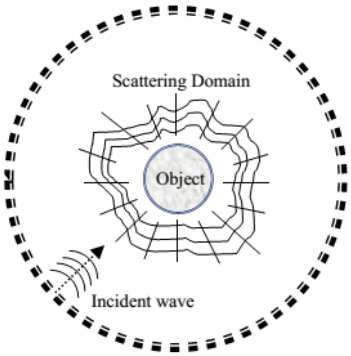

Fig. 1. Geometrical and acoustical configuration

Assuming that there is an infinite space containing homogeneous medium (M_1) such as water whose background wave number is k_0. There is also an object (M_2) with constant density and a wave number k(r) put inside this medium. The wave equation of the system can be shown as:

$$\nabla^2 p(\vec{r}) + k_0^2 p(\vec{r}) = -O(\vec{r})p(\vec{r}), \tag{1}$$

where

$$O(\vec{r}) = k_1^2 - k_0^2 - \rho(r)^{1/2}\nabla^2\rho(r)^{-1/2}, \tag{2}$$

$$k_1(r) = \frac{\omega}{c_1(r)} + i\alpha(r). \tag{3}$$

$k_1(r)$ is the wave number, $c_1(r)$ is the sound speed, $\alpha(r)$ is the attennuation, $\rho(r)$ is the density, and ω is the angular frequency.

The incident wave is denoted as $p^{inc}(r)$, the scattered wave can then be obtained as follows:

$$p^{sc}(r) = \int_\Omega O(r')p(r')G_0(k_0, r - r')\,dr' \tag{4}$$

where $p(r) = p^{inc}(r) + p^{sc}(r)$ is the total pressure inside the inhomogenerous area Ω and $G_0(k_0, r - r')$ is the Green's function. When the background is homogenerous, G_0 is the 0-th Hankel function of the first kind:

$$G_0(k_0, r - r') = \frac{-i}{4}H_0^{(1)}(k_0|r - r'|) = \frac{-i}{4}\sqrt{\frac{2}{\pi k_0|r-r'|}}e^{i(k_0|r-r'|-\pi/4)}. \tag{5}$$

The total pressure can be expressed as

$$p(r) = p^{inc}(r) + \int_\Omega O(r')p(r')G_0(k_0, r - r')\,dr' \tag{6}$$

One of the effective solutions to solve Eq. (6) by discreting is Method of Moment (MoM). The pressure in the grid points (see Fig.1) can be computed in vector form with size $N^2\times1$:

$$\bar{p} = \left(\bar{I} - \bar{C}.\,\mathrm{diag}(\bar{O})\right)p^{inc}. \tag{7}$$

The exterior points give scatter vector $N_tN_r\times1$:

$$\bar{p}^{sc} = \bar{B}.\,\mathrm{diag}(\bar{O}).\,\bar{p}\,, \tag{8}$$

where $\bar{B}$ is the matrix with Green's coefficient $G_0(r,r')$ from each pixel to the receiver, $\bar{C}$ is the matrix with Green's coefficient $G_0(r,r')$ among all pixels, $\bar{I}$ is identity matrix.

There are two unknown variables are $\bar{p}$ and $\bar{O}$ in equations (7) and (8). In this case, the first Born approximation has been applied and the forward equation (7) and (8) can be rewritten [9]:

$$\Delta p^{sc} = \bar{B}.\,\mathrm{diag}(\bar{p}).\,\Delta\bar{O} = \bar{M}.\,\Delta\bar{O}, \tag{9}$$

where $\bar{M} = \bar{B}.\,\mathrm{diag}(\bar{p})$. For each transmitter and receiver, we will have amatrix $\bar{M}$ and a scalar value Δp^{sc}. Realize that unkown vector $\bar{O}$ has $N \times N$ variables which are equal to the number of pixels in RIO. Object function can be estimated by iterations:

$$\bar{O}^n = \bar{O}^{(n-1)} + \Delta\bar{O}^{(n-1)}, \tag{10}$$

where $\bar{O}^n$ and $\bar{O}^{(n-1)}$ are object functions at present and previous steps, respectively; $\Delta\bar{O}$ can be estimated by solving Tikhonov regularization problem [10]:

$$\Delta\bar{O} = \arg\min_{\Delta\bar{O}}\left\|\Delta\bar{p}^{sc}{}_t - \bar{M}_t\Delta\bar{O}\right\|_2^2 + \gamma\|\Delta\bar{O}\|_2^2, \tag{11}$$

where $\Delta\bar{p}^{sc}$ is the $(N_tN_r \times 1)$ vector, contains the difference between predicted and measured scattered ultrasound signals; $\bar{M}_t$ is system matrix $(N_tN_r \times N^2)$ formed by N_tN_r different matrixes $\bar{M}_t$; and γ is the regularization parameter.

The DBIM procedure is presented in Algorithm 1.

Algorithm 1. The Distorted Born Iterative Method - DBIM

Choose initial values: $\bar{O}_{(n)} = \bar{O}_{(0)}$ and $\bar{p}_0 = \bar{p}^{inc}$ using (13)

For $n = 1$ *to* N_{sum}, **do**

1. Calculate $\bar{B}$ and $\bar{C}$
2. Calculate p, $\bar{p}^{sc}$ corresponding to $\bar{O}_{(n)}$ using (7, 8)
3. Calculate $\Delta\bar{p}^{sc}$ using (9)
4. Calculate $\Delta\bar{O}_{(n)}$ using (11)
5. Calculate $\bar{O}_{(n+1)} = \bar{O}_{(n)} + \Delta\bar{O}_{(n)}$

End For

III. The Pproposed Method

The complexity of the reconstruction system depends on the total number of iterations (N_{sum}), the number of transmitters (N_t) and receivers (N_r).

DBIM uses Born approximation to compute iterative solutions of a nonlinear inverse scattering problem. The Tikhonov regularization problem can be resolved directly or indirectly using an iterative method. However, the iterative method is more efficient than the direct one, especially when M is sparse or has a special form (e. g. , wavelet matrices or partial Fourier). In [11], M is determined by using multiple transmitters and detectors placed at equal distances. This configuration would make M become large, thus, it is not efficient for the iteration steps.

In this paper, we propose to use a uniform under-sampling configuration of detectors, with the number of detectors is smaller than that in the conventional configuration. With a reduced number of measurements (i.e., the size of M), and hence reduced the computational complexity in the iteration process, the proposed configuration maintains a quality of the reconstruction comparable to that obtained by the conventional configuration. Note that the transmitters are still placed at equal distance as in the conventional configuration.

Set $L = N \times N$ pixels, and define the sampling ratio

$$r = \frac{N_t N_r}{L^2} \tag{12}$$

When $N_t = N_r = L$, $r = 1$; this corresponds to the conventional configuration with full linear sampling. Otherwise, we have $r < 1$ and this corresponds to the under-sampling configuration. In practice, the value of maximum number of measurements depends on the accuracy of the mechanical system rotating around the object, which assembles the transmitters and detectors.

IV. Simulation And Results

Simulation parameters of scenarios are showed in Table 1. The full-sampling and under-sampling configurations are taken into account in the first and second-to-forth scenarios, respectively. In these scenarios, two objects whose sizes are 5mm and 2mm in diameter are considered in order to reconstruct in the inhomogeneous environment.

Table 2 shows the relationship between the number of measurements and variables of scenarios (i.e. the sampling ratio, r).

Table 1. Simulation parameters of scenarios

Parameters \ Scenarios	1	2	3	4
N_t	30	15	14	13
N_r	30	15	14	13
Other parameters	Frequency f = 1MHz; N = 30, N_{sum} = 8; Scattering area diameters are 5mm and 2mm, respectively; Sound contrast 5%; Gaussian noise 10%; Distances from transmitters and receivers to the center of the object are 100mm and 100mm, respectively.			

Table 2. The relationship between the number of measurements and variables of scenarios

Parameters \ Scenarios	1	2	3	4
Variables ($N \times N$)	900	900	900	900
Measurements ($N_t \times N_r$)	900	225	196	169
Measurements/ Variables (r)	1	0.25	0.22	0.19

The incident pressure for a Bessel beam of zero order in two-dimensional case is

$$\bar{p}^{inc} = J_0(k_0|r - r_k|), \tag{13}$$

where J_0 is the 0^{th} order Bessel function and $|r - r_k|$ is the distance between the transmitter and the k^{th} point in the ROI.

Fig. 2 shows the ideal object functions which are needed to reconstruct.

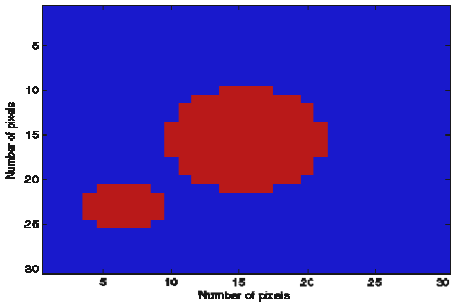

Fig. 2. Ideal object function

Figs. 3, 4 show the reconstructed results after the first iteration of the DBIM method in case of 900 measurements (i.e. $r = 1$) and SC-DBIM method in case of 225 measurements (i.e. $r = 0.25$). In spite of the very small number of measurements in the proposed method, it offers much faster convergence rate and noise-unaffected nature in comparison with the conventional method.

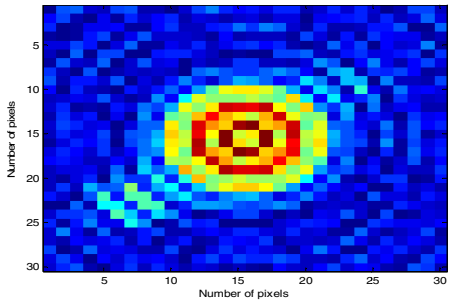

Fig. 3. The reconstructed result of the DBIM method after the first iteration (in case of 900 measurements, $r = 1$)

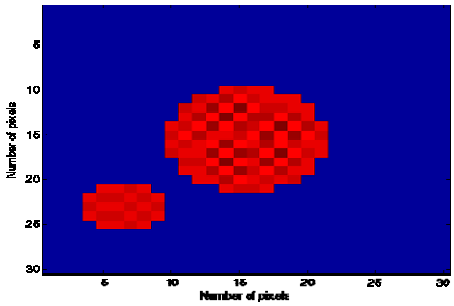

Fig. 4. The reconstructed result of the SC-DBIM method after the first iteration (in case of 225 measurements, $r = 0.25$)

Figs. 5, 6 show the reconstructed results of the DBIM method (after the eighth iteration) in case of 900 measurements (i.e. $r = 1$) and SC-DBIM method (after the second-to-eighth iteration) in case of 225 measurements (i.e. $r = 0.25$). It is clearly that the proposed method gets the high performance just after the second iteration. Meanwhile, the after-8-iteration reconstruction result of the conventional method is still significantly affected by noise, leading low convergence rate.

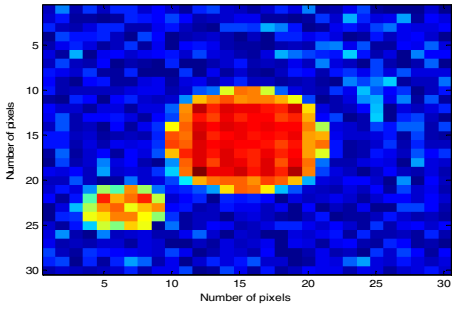

Fig. 5. The reconstructed result of the DBIM method after the eighth iteration (in case of 900 measurements, $r = 1$)

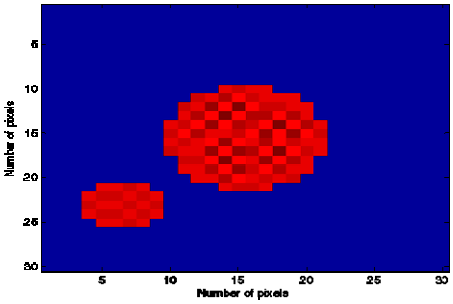

Fig. 6. The reconstructed result of the SC-DBIM method after the second-to-eighth iteration (in case of 225 measurements, $r = 0.25$)

To quantify the efficiency of the proposed approach, we acquire the object functions for a series of iterations. Then, the error in the reconstructed image is determined and compared to the original image in each iteration. Suppose that m is a $V \times W$ original image (i.e. ideal object function) and $\hat{m}$ is the reconstructed image. The normalized error can be defined as:

$$\varepsilon = \frac{1}{V \times W} \sum_{i=1}^{V} \sum_{j=1}^{W} \frac{\left| m_{ij} - \hat{m}_{ij} \right|}{\left| m_{ij} \right|} \tag{14}$$

Fig. 7 presents the error performance of the SC-DBIM method in comparison with the DBIM one. Some noted characteristics are below highlighted:

Firstly, for the full-sampling configuration (i.e. $r = 1$), with the same number of measurements (900), the normalized error and total runtime of the SC-DBIM method are 96.6% and 66.7% reduced, respectively. Interestingly, only 2 iterations is needed in the SC-DBIM method, while 8 iterations is used in the DBIM method. Therefore, we save the total runtime and number of iterations, but the much higher reconstruction quality. However, these are not what we concern due to using the large number of measurements which is not the outstanding feature of the sparse sampling problem.

Secondly, for the under-sampling configuration (i.e. $r < 1$), in spite of the very low sampling ratio ($r = 0.25$), the SC-DBIM method still get the very high performance, compared to the DBIM method with the high sampling ratio ($r = 1$). Namely, the normalized error and total runtime of the SC-DBIM method are 81.2% and 62.76% reduced, respectively.

Thirdly, for the acceptable reconstruction quality in the SC-DBIM method, the minimum sampling ratio is investigated in order to get the simplest measurement configuration of transducers. The simulation results indicate that the proposed method will get the high performance when $r \geq 0.22$.

Fourthly, for the total runtime of the DBIM and SC-DBIM methods, with the similar quality (i.e. DBIM with $r = 1$ and SC-DBIM with $r = 0.22$), the total runtime of the proposed method is 68.5% reduced, compared to the conventional method.

Table 1. The total runtime of the DBIM and SC-DBIM methods.

Methods	The total runtime
DBIM with $r = 1$	**761.240738 after 8 iterations**
SC-DBIM with $r = 1$	690.540757 after 8 iterations
	253.292221 after 2 iterations
SC-DBIM with $r = 0.25$	283.488239 after 8 iterations
SC-DBIM with $r = 0.22$	**239.744562 after 8 iterations**
SC-DBIM with $r = 0.19$	245.268858 after 8 iterations

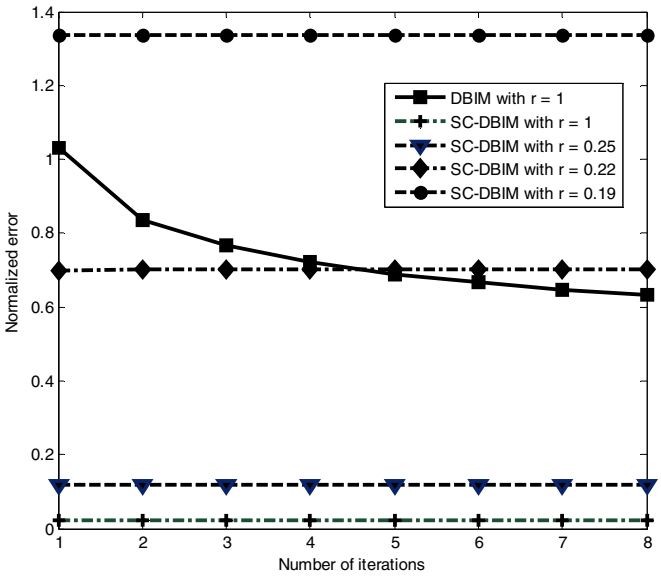

Fig. 7. Normalized error comparison of the DBIM and SC-DBIM methods

Table 1 shows the normalized error corresponding to different methods after each iteration.

V. CONCLUSIONS

Distorted Born iterative method, based on inverse scattering theory, is a common approach that can be used to detect the structures whose sizes are smaller than the wavelength of the incident wave, as opposed to the conventional method using echo information. This paper has successfully applied the simple uniform measurement configuration set-up of transducers and high-quality image reconstruction of l_1 non-linear regularization in order to improve the quality of the image reconstruction. This approach also provides a very simple set-up than others. So, it can avoid many types of measurement errors. Simulation scenarios of sound contrast reconstruction were implemented to demonstrate the very high performance of this scheme.

REFERENCES

[1] N. Duric, P. Littrup, A. Babkin, D. Chambers, S. Azevedo, A. Kalinin, R.Pevzner, M. Tokarev, E. Holsapple, O. Rama, and R. Duncan, Development of ultrasound tomography for breast imaging: Technical assessment, Medical Physics, vol. 32, no. 5, pp. 1375–1386, May 2005.

[2] C. Li, N. Duric, and L. Huang, reast imaging using transmission ultra-sound: Reconstructing tissue parameters of sound speed and attenuation, in International Conference on ioMedical Engineering and Informatics, vol. 2, 2008, pp. 708–712.

[3] J.-W. Jeong, T.-S. Kim, D. C. Shin, S. Do, M. Singh, and V. Z. Marmarelis, Soft tissue differentiation using multiband signatures of high resolution ul-trasonic transmission tomography, IEEE Transactions on Medical Imaging, vol. 24, no. 3, pp. 399–408, March 2005.

[4] S. A. Johnson, T. Abbott, R. Bell, M. Berggren, D. Borup, D. Robinson,J. Wiskin, S. Olsen, and . Hanover, Noninvasive breast tissue charac-terization using ultrasound speed and attenuation, in Acoustical Imaging, vol. 28, 2007, pp. 147–154.

[5] Devaney AJ (1982) Inversion formula for inverse scattering within the Born approximation. Optics Letters 7:111-112.

[6] Candès, Emmanuel J., Justin Romberg, and Terence Tao. "Robust uncertainty principles: Exact signal reconstruction from highly incomplete frequency information." Information Theory, IEEE Transactions on 52.2 (2006): 489-509.

[7] Donoho, David L. "Compressed sensing." Information Theory, IEEE Transactions on 52, no. 4 (2006): 1289-1306.

[8] Tran-Duc, Tan, Nguyen Linh-Trung, and M. N. Do. "Modified Distorted Born Iterative Method for Ultrasound Tomography by Random Sampling." In Communications and Information Technologies (ISCIT), 2012 International Symposium on, pp. 1065-1068. IEEE, 2012.

[9] R. J. Lavarello and M. L. Oelze: Tomographic Reconstruction of Three-Dimensional Volumes Using the Distorted Born Iterative Method. IEEE Transactions on Medical Imaging, 28, 2009, pp. 1643-1653.

[10] Gene H. Golub, Per Christian Hansen, and Dianne P. O'Leary: Tikhonov Regularization and Total Least Squares. SIAM Journal on Matrix Analysis and Applications. Vol. 21 Issue 1, Aug. 1999.

[11] Lavarello, Roberto, and Michael Oelze. "A study on the reconstruction of moderate contrast targets using the distorted Born iterative method."Ultrasonics, Ferroelectrics, and Frequency Control, IEEE Transactions on 55.1 (2008): 112-124.

[12] Kim, Seung-Jean, et al. "An interior-point method for large-scale l 1-regularized least squares." Selected Topics in Signal Processing, IEEE Journal of 1.4 (2007): 606-617.

Table 2. The normalized error after each iteration corresponding to different methods.

Iterations	1	2	3	4	5	6	7	8
Error of DBIM method (Scenario 1)	**1.0303**	**0.8347**	**0.7653**	**0.7208**	**0.6890**	**0.6658**	**0.6485**	**0.6341**
Comparison between the DBIM method in Scenario 1 and the SC-DBIM in Scenarios 2, 3, 4.								
Error of SC-DBIM (Scenario 1)	0.0218	0.0215	0.0215	0.0215	0.0215	0.0215	0.0215	0.0215
% Reduced error	98%	97.42%	97.2%	97%	96.88%	96.77%	96.6%	96.6%
Error of SC-DBIM (Scenario 2)	0.1194	0.1194	0.1194	0.1194	0.1194	0.1194	0.1194	0.1194
% Reduced error	88.4%	85.7%	84.4%	83.4%	82.67%	82.1%	81.6%	81.2%
Error of SC-DBIM (Scenario 3)	0.7000	0.7001	0.7001	0.7001	0.7001	0.7001	0.7001	0.7001
% Reduced error	32%	16.12%	8.52%	2.87%	1.59%	4.89%	7.4%	10.4%
Error of SC-DBIM (Scenario 4)	1.3369	1.3370	1.3370	1.3370	1.3370	1.3370	1.3370	1.3370
% Increased error	23%	37.6%	42.7%	46.1%	48.5%	50.2%	51.5%	52.6%